Treatment with Halofuginone Results in Marked Growth Inhibition of a von Hippel-Lindau Pheochromocytoma *in Vivo*

David J. Gross,[1] Israel Reibstein, Lola Weiss, Shimon Slavin, Hagit Dafni, Michal Neeman, Mark Pines, and Arnon Nagler

Endocrinology and Metabolism Service [D. J. G.] and Department of Bone Marrow Transplantation and Cancer Immunobiology [I. R., L. W., S. S.], Hadassah University Hospital, Jerusalem 91120; Department of Biological Regulation, Weitzmann Institute of Science, Rehovot 76100 [H. D., M. N.]; Institute of Animal Science, The Volcani Center, Bet Dagan [M. P.]; and Department of Bone Marrow Transplantation, Sheba Medical Center, Tel-Hashomer [A. N.], Israel

ABSTRACT

Halofuginone has recently been shown to inhibit tumor progression of various types of cancers. The antitumoral effect was associated with decreased tumor angiogenesis rather than a direct cytostatic effect on the tumor cells. The antiangiogenic action of the drug could be related to its inhibition of collagen type I synthesis, inhibition of matrix metalloproteinases (MMPs), or via both mechanisms because both collagen synthesis and MMP activity have been shown to be involved in angiogenesis. Vascular endothelial growth factor (VEGF), in addition to its effect on endothelial cell proliferation, has been shown to be a potent inducer of MMP expression. Because von Hippel-Lindau (VHL)-associated tumors express high levels of VEGF, it was of interest to ascertain the potential usefulness of halofuginone for treatment of these tumors. Pheochromocytoma tissue fragments obtained at surgery from a VHL type 2a patient were propagated s.c. in male BALB/c *nu/nu* (nude) mice. For experiments, 2–3-mm tumor fragments were transplanted secondarily s.c. to nude mice. Two treatment groups received halofuginone in standard lab chow at 3 and 5 ppm; control animals received regular chow. All groups were followed for 6 weeks after transplantation. A marked and significant diminution of tumor size and weight was observed in the drug-treated animals (>90% reduction of mean tumor volume for both the 3 and 5 ppm groups). *In vivo* magnetic resonance imaging analysis of tumors in halofuginone-treated animals showed a significant reduction of vascular functionality. Immunohistochemical studies revealed decreased collagen type I levels and vascular density in treated tumors and gelatinase assays of tumor extracts revealed a reduction of MMP-2 and MMP-9 activity in halofuginone-treated cells. Taken together, our data indicate that therapy directed at blocking MMP activity (presumably related to excessive VEGF expression in VHL) and reduction of type I collagen deposition curtails angiogenesis and thereby presumably tumor growth in this model system.

INTRODUCTION

VHL[2] disease is an autosomal dominant cancer syndrome characterized clinically by retinal angiomas, cerebellar and spinal cord hemangioblastomas, RCCs, pheochromocytomas, and less commonly, pancreatic islet cell tumors and epididymal cysts. This multiorgan involvement can appear in various combinations; however, in an affected kindred, the clinical manifestations of the disease are usually invariable and breed true. The gene associated with VHL has been cloned, and germ-line mutations in the *VHL* gene can be detected in virtually all patients with VHL: these can be micro- and macrodeletions or point mutations scattered throughout all three exons of the VHL gene. The *VHL* gene encodes a 213 amino acid peptide, pVHL. pVHL, considered to be a tumor suppressor gene, has pleotropic effects in the cell, the most prominent being the lack of cellular responsiveness to ambient oxygen tension. Thus, it has been shown that in tumor cell lines derived from VHL patients, mutated pVHL is associated with constitutively elevated VEGF mRNA, unresponsive to normal normoxia/hypoxia regulation. Reintroduction of wild-type pVHL results in restoration of VEGF regulation and inhibition of tumor growth *in vivo* (for review see Ref. 1). Thus, mutated pVHL-related overexpression of VEGF and its receptors in the well-vascularized VHL tumors might implicate unregulated VEGF-induced angiogenesis as a major pathogenetic pathway, leading toward tumor formation in this disease. We have recently shown that the antiangiogenic agent linomide significantly inhibits the growth of VHL pheochromocytoma explants in nude mice (2). This effect was found to be associated with decreased tumor vascularity and VEGF mRNA levels. Our data indicated that in VHL disease, therapy directed at abrogation of the effect of constitutively expressed VEGF may constitute an effective medical treatment. Because the clinical use of linomide is precluded by unacceptable toxicity in human subjects (3), we sought an alternative antiangiogenic approach. Halofuginone has recently been shown to inhibit tumor progression of C6 glioma, bladder carcinoma, and prostate tumors (4–6). In these tumors, a correlation between the inhibition of tumor growth and reduction in collagen type I synthesis was observed. This antitumoral effect has been shown

Received 1/7/03; revised 4/7/03; accepted 4/9/03.
The costs of publication of this article were defrayed in part by the payment of page charges. This article must therefore be hereby marked *advertisement* in accordance with 18 U.S.C. Section 1734 solely to indicate this fact.

[1] To whom requests for reprints should be addressed, at Present address: Institute of Endocrinology and Metabolism, Rabin Medical Center, (Beilinson Campus), Petach-Tikva 49100, Israel. Phone: 972-3-9377184; Fax: 972-3-9211403; E-mail: gross@vms.huji.ac.il.

[2] The abbreviations used are: VHL, von Hippel-Lindau; MMP, matrix metalloproteinase; VEGF, vascular endothelial growth factor; MRI, magnetic resonance imaging; ECM, extracellular matrix; EC, endothelial cell; RCC, renal cell carcinoma.

to be associated with an inhibitory effect of the drug on various stages of angiogenesis (7). The aim of our study was to assess the potential usefulness of halofuginone for treatment of VHL-related tumors. This is of particular interest because these tumors have a rich vascular bed presumably related to the characteristically high levels of VEGF expression.

MATERIALS AND METHODS

Materials

FCS, DMEM, and trypsin-EDTA solution (0.25–0.02%) were obtained from Biochemical Industries (Bet-HaEmek, Israel). Sirius red F3B was obtained from BDH Laboratory Supplies (Poole, United Kingdom). A rat collagen a1(I) 1600-bp probe was a generous gift from Barbara E. Kream (University of Connecticut). Halofuginone bromhydrate was obtained from Collgard Biopharmaceuticals Ltd. (Tel Aviv, Israel).

Methods

Establishment of a Transplantable VHL Tumor Line. Paraganglioma tissue fragments obtained at surgery from a patient with VHL type 2A (harboring a missense mutation, resulting in replacement of Val by Phe at position 166 of the VHL protein; Ref. 8) were transplanted s.c. to male BALB/c *nu*/*nu* (nude) mice. In 4 of 20 mice, tumors appeared after ~7 months. Tissue fragments obtained from these 4 mice were secondarily transplanted s.c. to nude mice. Tumors were identified as originating from the original chromaffin tumor by positive stains for chromogranin A and neuron-specific enolase (data not shown). All animal experiments were conducted according to the stipulations of the local Animal Care Committee.

Treatment Groups. For prevention experiments, fragments 2–3 mm in diameter were implanted s.c. under the neck skinfold of nude mice. For intervention, the fragments were allowed to grow to 1 cm in diameter before initiation of therapy. Treatment groups received halofuginone in standard lab chow at 3 and 5 ppm; control animals received regular chow. In some experiments, halofuginone was administered i.p (1 μg/animal/day × 6 days/week). All groups were followed for 6 weeks after transplantation.

Assessment of the Effect of Halofuginone Therapy on Tumor Growth at Termination of Experiments. Before tumor excision, animals were anesthetized, and tumor volume was calculated as follows: the maximal tumor diameter (*x* axis) and two additional diameters bisecting the *x* axis in the *y* and *z* axes were measured. The mean value of these three parameters served as an average value for calculation of the tumor volume. Tumors were then removed, weighed, and samples were processed for histopathological examination and for gelatinase activity. In some experiments, *in vivo* MRI assessment of tumor vascularity was also performed.

Tumor Collagen Expression. Tissue samples were collected and fixed overnight in 4% paraformaldehyde in PBS at 48°C. Serial 5-mm sections were prepared after the samples had been dehydrated in graded ethanol solutions, cleared in chloroform, and embedded in Paraplast. Differential staining of collagenous and noncollagenous proteins was performed with 0.1% sirius red, with 0.1% fast green as a counterstain, in saturated picric acid. By this procedure, collagen is stained red (9). For hybridization, the sections were deparaffinized in xylene, rehydrated through a graded series of ethanol solutions, rinsed in distilled water (5 min), and incubated in 2× SSC solution at 70°C for 30 min. The sections were then rinsed in distilled water and treated with proteinase [0.125 mg/ml in 50 mM Tris HCl, 5 mM EDTA (pH 7.5)] for 10 min. After digestion, the slides were rinsed with distilled water, postfixed in 10% formalin in PBS, blocked in 0.2% glycine, rinsed in distilled water, rapidly dehydrated through graded ethanol solutions, and air-dried for several hours. Before hybridization, the 1600-bp rat collagen a1(I) insert was cut out from the original plasmid (pUC18) and inserted into pSafyre. The sections were hybridized with digoxigenin-labeled collagen a1(I) probe (10). All of the preparations for *in situ* hybridization within each experiment were performed simultaneously with the same probe, and all sections were dipped in emulsion and exposed for the same length of time. No signal was observed with the sense probe.

Zymography. Dispersed pheochromocytoma cells were seeded into 35-mm culture plates (2.5×10^5 cells/plate) and maintained for 24 h in DMEM supplemented with 10% FCS. Subconfluent cell cultures were incubated for 24 h in the absence or presence of increasing concentrations (20–200 ng/ml) of halofuginone, and aliquots of the resultant conditioned medium were analyzed for gelatinolytic activity. Conditioned medium of human melanoma SB-2 cells expressing both MMP-2 and MMP-9 was used as a positive control. MMP-2 activity was determined on gelatin-impregnated (1 mg/ml; Difco, Detroit, MI) SDS-8% polyacrylamide gels, as described previously (11). Briefly, samples of the culture media, normalized for equal cell protein, were separated on the substrate-impregnated gels under nonreducing conditions, followed by 30-min incubation in 2.5% Triton X-100 (Sigma, St. Louis, MO). The gels were then incubated for 16 h at 37°C in 50 mM Tris, 0.2 M NaCl, 5 mM $CaCl_2$, 0.02% Brij 35 (w/v) at pH 7.6. At the end of the incubation period, the gels were stained with 0.5% Coomassie Blue G 250 (Bio-Rad, Richmond, CA) in methanol/acetic acid/H_2O (30:10:60).

MRI Assessment of Tumor Vasculature. MRI experiments were performed on a horizontal 4.7 T Bruker Biospec spectrometer using an actively radio frequency-decoupled surface coil, 2 cm in diameter, embedded in a Perspex board and a birdcage transmission coil. Mice were anesthetized (75 mg/kg Ketamine +3 mg/kg Xylazine, i.p.) and placed supine with the tumor located on the center of the surface coil. MRI data were analyzed on a Indigo-2 work station (Silicon Graphics, USA) using Paravision software (Bruker, Germany).

Vascular function (VF) was derived from images acquired during inhalation of carbogen (95% oxygen 5% CO_2) and air-CO_2 (95% air 5% CO_2; equation 1):

$$VF = b\Delta Y = \frac{\ln(I_{carbogen}/I_{air-CO_2})}{TE \times C_{MRI}} \quad (1)$$

where *TE* is the echo time, *Y* is the fraction of oxyhemoglobin, *b* is the volume fraction of blood, and $C_{MRI} = 599\ s^{-1}$ at 4.7 T (12). This parameter measures the capacity of erythrocyte-mediated oxygen delivery from the lungs to each pixel in the image (12, 13).

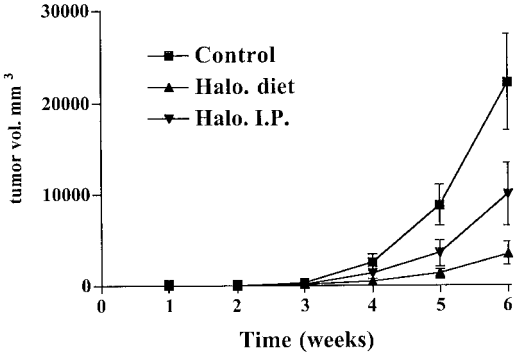

Fig. 1 The effect of oral (3 ppm in chow) and i.p. (1 μg/mouse) halofuginone on tumor volume in nude mice implanted with VHL-derived paraganglioma. Tumor tissue fragments of 2–3 mm in size were implanted s.c. under the neck skinfold, and animals ($n = 10$ for each group) were started on the treatments at day −5 (at 6 weeks control *versus* diet, $P < 0.002$; control *versus* i.p., $P = 0.06$). Data are expressed as mean ± SE, representative of three qualitatively similar experiments.

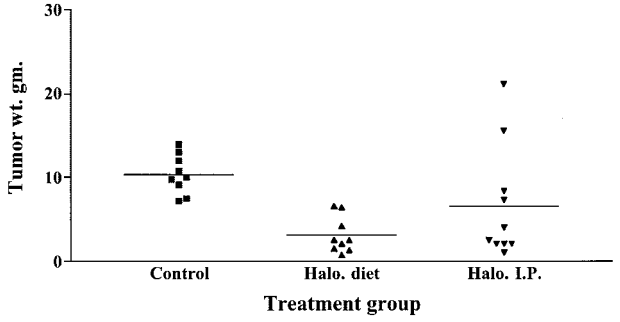

Fig. 2 The effect of oral and i.p. halofuginone on tumor weight in nude mice implanted with VHL-derived paraganglioma. The figure shows the wet weights of the tumors at the end of the experiment depicted in Fig. 1 (control *versus* oral, $P < 0.0001$; control *versus* i.p. not significant; *horizontal line* depicts mean weight for each group).

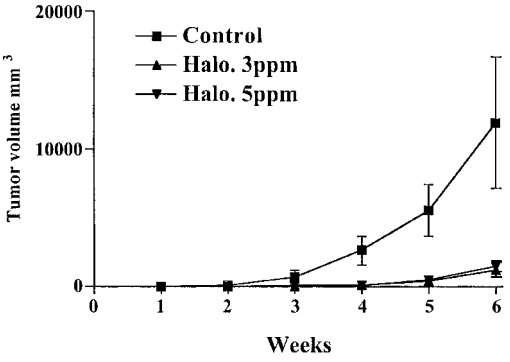

Fig. 3 The effect of two different doses of oral halofuginone (3 and 5 ppm in chow) on tumor volume in nude mice implanted with VHL-derived paraganglioma. Tumor tissue fragments of 2–3 mm in size were implanted s.c. under the neck skinfold, and animals ($n = 10$ for each group) were started on the treatments at day −5 (at 6 weeks control *versus* 3 and 5 ppm, $P < 0.002$). Data are expressed as mean ± SE.

Vascular reactivity was derived from air and air CO_2 images (equation 2):

$$\mathrm{VD} = \frac{\ln(I_{\mathrm{air}-\mathrm{CO}_2}/I_{air})}{TE \times C_{\mathrm{MRI}}}. \qquad (2)$$

Positive VD corresponds to increased signal intensity by hypercapnia because of elevated blood oxygenation (and/or increase blood flow), whereas vascular steal will result in negative VD values (12).

Statistical Analysis. Group comparisons were performed using Students' two tailed *t* test.

RESULTS

Inhibition of Tumor Progression by Halofuginone. Animals administered with either halofuginone 3 ppm in the chow or 1 μg/animal/day i.p. daily, commencing at day −5 with respect to the time of transplantation (prevention experiment), showed marked retardation of tumor growth as compared with control animals (Fig. 1). This inhibition of tumor growth was also reflected by a significant difference in tumor weights at the end of the experiment (Fig. 2). Because oral administration in chow was more effective and uniform (Fig. 1), subsequent experiments were performed with the oral preparation. Fig. 3 shows the dose dependence of oral halofuginone with respect to inhibition of tumor growth; 3 ppm was effective as 5 ppm and caused less loss of weight than the higher dose (23.8 ± 1.2 and 20.6 ± 1.0 g, respectively, $P = 0.055$). We also performed intervention experiments in which the tumors were allowed to attain 1 cm in diameter, at which time, halofuginone treatment was started at the 3 ppm in chow. In these experiments, there was a tendency for retardation of tumor progression, but this did not achieve statistical significance (data not shown).

Assessment of Whole Tumor Vasculature by MRI. To assess whole tumor vascularity and *in vivo* vascular function, we performed MRI analysis of tumors at the end point of a prevention experiment. We analyzed VF and vasoreactivity/vascular maturation (VD) in a region of interest within the tumors. The halofuginone-treated tumors have extremely poor VF inside the tumors, relative to control tumors (Fig. 4; $P < 0.02$, unpaired two-tailed *t* test). No differences in tumor VD were observed between treated and control animals (data not shown).

The Effect of Halofuginone on Tumor Collagen a1(I). Cells within the control xenografts expressed high levels of the collagen a1(I) gene resulted in high levels of collagen fibers as demonstrated by *in situ* hybridization and Sirius red staining. In contrast, halofuginone treatment caused reduction in the collagen a1(I) gene expression and reduction in collagen fibers in agreement with its mode of action (data not shown).

The Effect of Halofuginone on Tumor MMP Activity. We investigated the effect of halofuginone on MMP gelatinolytic activity of the pheochromocytoma cells *in vitro*. For these studies, subconfluent cultures of dispersed cells were treated for 24 and 48 h with increasing concentrations (20–200 ng/ml) of halofuginone in the medium. Aliquots of the conditioned medium were applied onto gelatin-embedded SDS-polyacrylamide gels. The zymogram shown in Fig. 5 demonstrates that the gelatinolytic activity of MMP-2 and MMP-9 activity was mark-

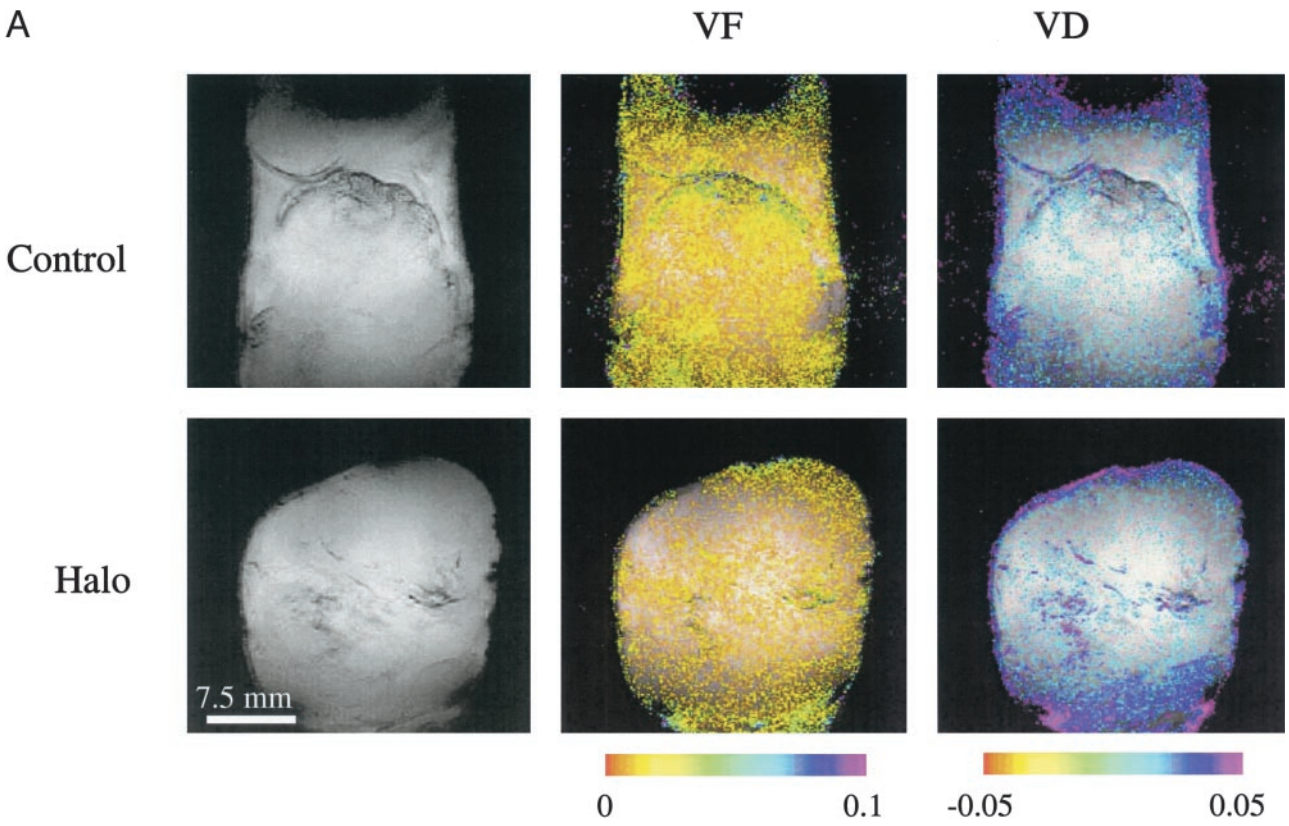

Fig. 4 MRI analysis of the effects of halofuginone (3 ppm) on tumor VF. *A*, representative images and VF and VD maps of treated and control tumors. *B*, the mean values of VF are denoted in arbitrary units ± SD (control *versus* halofuginone, $P < 0.02$). VF values were obtained from three separate experiments (3 treated + 3 control in the first two experiments and 4 treated + 4 control in the third). VF values were first averaged for each mouse (in regions of interest containing the tumor in three to five slices) and then averaged for control ($n = 10$) and for treated ($n = 10$) groups. Data were acquired at 4.7 T on a Bruker Biospec spectrometer (Gradient echo imaging; TE = 10 ms; TR = 230 ms; slice thickness, 1 mm; inplane resolution, 117 μm). TE, time to echo; TR, time to relaxation.

edly reduced by halofuginone. Densitometric analysis of the zymograms revealed a >75% inhibition of MMP-2 activity in cells pretreated with 100 ng/ml halofuginone and virtually complete inhibition of MMP-9 activity.

DISCUSSION

We have shown that the growth of a VHL phechromocytoma xenografted to nude mice is markedly inhibited by halofuginone. In similar models, halofuginone has recently been shown to inhibit tumor progression of C6 glioma, bladder carcinoma, and prostate cancer (4–6). The antitumoral effect demonstrated in these studies appears to be related to decreased tumor angiogenesis rather than a direct cytostatic effect of the compound on the tumor cells. In keeping with these findings, in the present study, we found that the antitumoral effect of the compound is associated with marked decrease in tumoral vas-

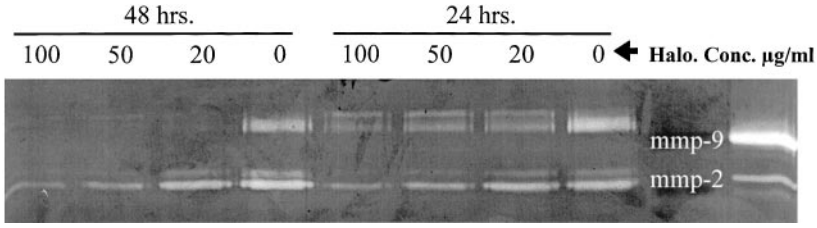

Fig. 5 Effect of halofuginone on MMP-2 gelatinolytic activity in cell-conditioned medium. Subconfluent-dispersed pheochromocytoma cells were incubated (24 and 48 h, 37°C) in the absence and presence of increasing concentrations of halofuginone in the medium. Aliquots (30–40 μl) of the incubation media were normalized for equal cell protein and applied for zymography on gelatin impregnated SDS-PAGE, as described in "Materials and Methods." Medium conditioned by SB-2 human melanoma cells (SB-2 CM), expressing both MMP-2 and MMP-9, was used as a positive control. Representative of $n = 2$ quantitatively similar experiments.

cularity, predominantly that of immature vessels, indicating a probable antiangiogenic mode of action. Once a tumor vascular bed is established, however, the effect of the drug is reduced, as exemplified by the diminished effect on tumor progression in intervention experiments. VHL-related tumors are characterized by enhanced expression of VEGF, which underlies the hypervascular phenotype of these tumors. Indeed, we have shown previously that abrogation of VEGF induced angiogenesis in this tumor type results in a marked antitumoral effect (2). Recently VEGF, in addition to its effect on EC proliferation, has been shown to be a potent inducer of MMP expression by vascular smooth muscle cells (14), both actions have been shown to be involved in angiogenesis (7). We have shown that the antiangiogenic effect of halofuginone is associated with both inhibition of collagen type I synthesis and inhibition of MMP activity; in contrast to the effect of linomide in this model system (2), no decrease of tumor VEGF mRNA was observed (data not shown).

The growth of new capillaries from preexisting blood vessels is dependent on the ECM that provides a complex combination of insoluble molecules that in concert with soluble growth factors and intercellular contacts modulate gene expression and consequently cell functions (15). Collagen type I, the major ECM component, plays an important role in the proliferation and invasion of the EC required for angiogenesis (16, 17). A marked increase in the transcription of type I collagen was demonstrated in ECs undergoing angiogenesis (18), and blockage of collagen secretion inhibited EC migration (19). Capillary ECs reorganize into a network of branching and anastomozing capillary-like tubes when sandwiched between two layers of type I collagen gel (20). When the collagen type I fibrils make contact with the apical side of the endothelium, they act as a stimulus to provide a template for vascular tube formation (21). Integrin (22) and nonintegrin (23) transmembrane receptors that exhibit specificity for collagen types have been identified in various tissues. The receptors for the native collagen the $\alpha 1\beta 1$ and $\alpha 2\beta 1$ integrins and are highly expressed by ECs during angiogenesis, and antibodies that block these receptors selectively inhibit VEGF-driven angiogenesis without affecting preexisting vasculature (24) Type I but not type IV collagen was found to regulate the expression of genes involved in ECs tube formation (25).

The MMP family plays an important role in the degradation of ECM in various physiological and pathological conditions. Accumulated evidence has suggested that MMPs contribute to cancer cell invasion of the surrounding normal tissues and metastasis through the cell surface ECM degradation. Strong correlations have been reported between elevated MMP levels and various tumor cell invasiveness such as gliomas (26) Among them, attention has been focused on gelatinases MMP-2 and MMP-9. Previously, halofuginone was demonstrated as an inhibitor of MMP-2 (11), and in this study, we demonstrated that it inhibited the activity of MMP-9 as well.

In this study, halofuginone treatment did not cause tumor regression and was more effective as a chemopreventive rather than as a chemotherapeutic modality of treatment. The drug dosage and route of administration used in this study appears to be appropriate for achieving maximal therapeutic effect because neither increasing the drug dosage nor parenteral administration did not improve drug efficacy. Patients at risk for VHL disease (*i.e.,* carriers of VHL gene germ-line mutations) are subject to lifelong tumor surveillance because of the high penetrance of the various tumor phenotypes in such mutation carriers. Therefore, it is expected that such VHL-related tumors will be detected very early in the future at a clinical stage at which medical rather than surgical therapy might be contemplated. For example, VHL patients who develop RCC are not operated immediately but are followed by imaging and undergo tumor resection with nephron-sparing surgery only when the tumor size exceeds 3 cm in diameter (27). The rationale for this clinical approach is the relative benign course of small tumors on the one hand (<3 cm in diameter) and the inevitable need for recurrent surgery because of multicentricity of RCC in VHL patients, on the other (28). In this setting, the antiangiogenic effect of halofuginone could prove effective in inhibition of RCC growth and possibly arrest tumor progression at a relatively early and indolent stage. Our findings require validation in other VHL tumor types, namely RCC and central nervous system hemangioblastomas, because management of these tumors is most likely to benefit from early antiangiogenic therapy.

In conclusion, our studies show that halofuginone therapy shows promise for hitherto medically untreatable VHL disease. This experimental system could serve as paradigm for treatment of other cancers in which VEGF-driven angiogenesis plays a role in the pathogenesis of the disease. Halofuginone is one of a very few antiangiogenic factors that can be p.o. administered, which makes such a therapy clinically attractive. Thanks to its low molecular weight, it can be easily synthesized in large

quantities under clinical pharmaceutical guidelines. Moreover, angiogenesis inhibitors are less likely to induce resistance than treatments that target tumor cells, therefore, it might be permissible to use such antiangiogenic factors in long-term maintenance therapy.

REFERENCES

1. Clifford, S. C., and Maher, E. R. Von Hippel-Lindau disease: clinical and molecular perspectives. Adv. Cancer Res., *82:* 85–105, 2001.

2. Gross, D. J., Reibstein, I., Weiss, L., Slavin, S., Stein, I., Neeman, M., Abramovitch, R., and Benjamin, L. E. The antiangiogenic agent linomide inhibits the growth rate of von Hippel-Lindau paraganglioma xenografts to mice. Clin. Cancer Res., *5:* 3669–3675, 1999.

3. Schwid, S. R., and Trotter, J. L. Lessons from linomide: a failed trial, but not a failure. Neurology, *54:* 1716–1717, 2000.

4. Abramovitch, R., Dafni, H., Neeman, M., Nagler, A., and Pines, M. Inhibition of neovascularization and tumor growth, and facilitation of wound repair, by halofuginone, an inhibitor of collagen type I synthesis. Neoplasia, *1:* 321–329, 1999.

5. Elkin, M., Ariel, I., Miao, H. Q., Nagler, A., Pines, M., de-Groot, N., Hochberg, A., and Vlodavsky, I. Inhibition of bladder carcinoma angiogenesis, stromal support, and tumor growth by halofuginone. Cancer Res., *59:* 4111–4118, 1999.

6. Gavish, Z., Pinthus, J. H., Barak, V., Ramon, J., Nagler, A., Eshhar, Z., and Pines, M. Growth inhibition of prostate cancer xenografts by halofuginone. Prostate, *51:* 73–83, 2002.

7. Elkin, M., Miao, H. Q., Nagler, A., Aingorn, E., Reich, R., Hemo, I., Dou, H. L., Pines, M., and Vlodavsky, I. Halofuginone: a potent inhibitor of critical steps in angiogenesis progression. FASEB J., *14:* 2477–2485, 2000.

8. Gross, D. J., Avishai, N., Meiner, V., Filon, D., Zbar, B., and Abeliovich, D. Familial pheochromocytoma associated with a novel mutation in the *von Hippel-Lindau* gene. J. Clin. Endocrinol. Metab., *81:* 147–149, 1996.

9. Gascon-Barre, M., Huet, P. M., Belgiorno, J., Plourde, V., and Coulombe, P. A. Estimation of collagen content of liver specimens. Variation among animals and among hepatic lobes in cirrhotic rats. J. Histochem. Cytochem., *37:* 377–381, 1989.

10. Bruck, R., Genina, O., Aeed, H., Alexiev, R., Nagler, A., Avni, Y., and Pines, M. Halofuginone to prevent and treat thioacetamide-induced liver fibrosis in rats. Hepatology, *33:* 379–386, 2001.

11. Elkin, M., Reich, R., Nagler, A., Aingorn, E., Pines, M., de-Groot, N., Hochberg, A., and Vlodavsky, I. Inhibition of matrix metalloproteinase-2 expression and bladder carcinoma metastasis by halofuginone. Clin. Cancer Res., *5:* 1982–1988, 1999.

12. Abramovitch, R., Frenkiel, D., and Neeman, M. Analysis of subcutaneous angiogenesis by gradient echo magnetic resonance imaging. Magn. Reson. Med., *39:* 813–824, 1998.

13. Abramovitch, R., Dafni, H., Smouha, E., Benjamin, L. E., and Neeman, M. *In vivo* prediction of vascular susceptibility to vascular susceptibility endothelial growth factor withdrawal: magnetic resonance imaging of C6 rat glioma in nude mice. Cancer Res., *59:* 5012–5016, 1999.

14. Wang, H., and Keiser, J. A. Vascular endothelial growth factor up-regulates the expression of matrix metalloproteinases in vascular smooth muscle cells: role of flt-1. Circ. Res., *83:* 832–840, 1998.

15. Lukashev, M. E., and Werb, Z. ECM signalling: orchestrating cell behaviour and misbehaviour. Trends Cell Biol., *8:* 437–441, 1998.

16. Iruela-Arispe, M. L., Hasselaar, P., and Sage, H. Differential expression of extracellular proteins is correlated with angiogenesis *in vitro*. Lab. Investig., *64:* 174–186, 1991.

17. Sage, E. H., and Vernon, R. B. Regulation of angiogenesis by extracellular matrix: the growth and the glue. J. Hypertens. Suppl., *12:* S145–S152, 1994.

18. Iruela-Arispe, M. L., Diglio, C. A., and Sage, E. H. Modulation of extracellular matrix proteins by endothelial cells undergoing angiogenesis *in vitro*. Arterioscler. Thromb., *11:* 805–815, 1991.

19. Madri, J. A., and Stenn, K. S. Aortic endothelial cell migration. I. Matrix requirements and composition. Am. J. Pathol., *106:* 180–186, 1982.

20. Montesano, R., Orci, L., and Vassalli, P. *In vitro* rapid organization of endothelial cells into capillary-like networks is promoted by collagen matrices. J. Cell Biol., *97:* 1648–1652, 1983.

21. Jackson, C. J., and Jenkins, K. L. Type I collagen fibrils promote rapid vascular tube formation upon contact with the apical side of cultured endothelium. Exp. Cell Res., *192:* 319–323, 1991.

22. Heino, J. The collagen receptor integrins have distinct ligand recognition and signaling functions. Matrix Biol., *19:* 319–323, 2000.

23. Shrivastava, A., Radziejewski, C., Campbell, E., Kovac, L., McGlynn, M., Ryan, T. E., Davis, S., Goldfarb, M. P., Glass, D. J., Lemke, G., and Yancopoulos, G. D. An orphan receptor tyrosine kinase family whose members serve as nonintegrin collagen receptors. Mol. Cell, *1:* 25–34, 1997.

24. Senger, D. R., Claffey, K. P., Benes, J. E., Perruzzi, C. A., Sergiou, A. P., and Detmar, M. Angiogenesis promoted by vascular endothelial growth factor: regulation through $\alpha 1\beta 1$ and $\alpha 2\beta 1$ integrins. Proc. Natl. Acad. Sci. USA, *94:* 13612–13617, 1997.

25. Regazzoni, C., Winterhalter, K. H., and Rohrer, L. Type I collagen induces expression of bone morphogenetic protein receptor type II. Biochem. Biophys. Res. Commun., *283:* 316–322, 2001.

26. Nakada, M., Okada, Y., and Yamashita, J. The role of matrix metalloproteinases in glioma invasion. Front Biosci., *8:* E261–E269, 2003.

27. Maher, E. R., and Kaelin, W. G., Jr. von Hippel-Lindau disease. Medicine (Baltimore), *76:* 381–391, 1997.

28. Walther, M. M., Lubensky, I. A., Venzon, D., Zbar, B., and Linehan, W. M. Prevalence of microscopic lesions in grossly normal renal parenchyma from patients with von Hippel-Lindau disease, sporadic renal cell carcinoma and no renal disease: clinical implications. J. Urol. *154:* 2010–2014, 1995.